IDENTIFYING GROUP-WISE CONSISTENT SUB-NETWORKS VIA SPATIAL SPARSE REPRESENTATION OF NATURAL STIMULUS FMRI DATA

Cheng Lyu[1,2], Xiang Li[2], Jinglei Lv[1,2], Xintao Hu[1], Junwei Han[1], Lei Guo[1], Tianming Liu[2]

[1]School of Automation, Northwestern Polytechnical University, Xi'an, China
[2]Cortical Architecture Imaging and Discovery Lab, Department of Computer Science and Bioimaging Research Center, The University of Georgia, GA, USA

ABSTRACT

Natural stimulus fMRI has been increasingly used in the brain imaging and brain mapping fields thanks to its more realistic stimulation of the brain's perceptive and cognitive systems. However, identifying consistent functional networks across different brains in natural stimulus fMRI data has been challenging due to the intrinsic variability of individual brain's responses and a variety of sources of noises. Inspired by recent promising results of sparse representation of whole-brain fMRI data, in this paper, we present a novel hybrid temporal and spatial sparse representation of whole-brain natural stimulus fMRI data for the inference of common functional networks across fMRI sessions and individual brains. Experimental results on natural stimulus fMRI dataset demonstrated the effectiveness of this framework.

Index Terms—consistent brain network, natural stimulus, sparse coding, fMRI .

1. INTRODUCTION

In neuroimaging studies, block-based task experiments have been widely used in mapping functional brain locations [1]. However, recently, researchers more and more utilize real-life stimuli such as images (e.g. [2]), video streams (e.g. [3]) or audio excerpts (e.g. [4]) for natural stimulus fMRI. In general, natural stimulus contains more complex and dynamic content than simply-repeated task-based experiments, and it is considered as more reliable to stimulate functional responses of the human brain to real-world situation [5].

However, despite the increasingly wider applications of natural stimulus fMRI in the brain mapping field, data modeling and analysis methods have mainly relied on traditional methods such as independent component analysis (ICA) [6], general linear model (GLM) [7], inter-subject correlation (ISC) [8]. Recent relatively novel methods such as brain network modeling have been largely underexplored in natural stimulus fMRI data, though they have been extensively studied in task-based fMRI and resting state fMRI data. In our perspective, the main difficulty might lie in the complex and multiple concurrent brain networks that interact with each other during natural stimulus fMRI scans [9].

Recently, Lv et al., [10, 11] presented a novel framework of sparse representation of whole-brain fMRI signals for inference of concurrent task-evoked and resting state brain networks and demonstrated promising results. The basic idea is to represent functional network activities by the learned time-series dictionary atoms that can well reconstruct whole-brain fMRI signals under a sparsity constraint. One of the prominent advantages of this framework is that many meaningful networks and their interactions can be simultaneously inferred. Inspired by the success of sparse representation of whole-brain fMRI signals [10, 11], in this paper, we present a novel hybrid temporal and spatial sparse representation framework to infer consistent networks across fMRI scan sessions and across different brains. In comparison with prior sparse representation methods, the key new methodological contribution here is that the first stage of temporal sparse representation will generate variable temporal dictionaries, but their coefficients' spatial patterns are relatively more regularly distributed. Then, we apply the second stage of spatial sparse representation to infer those spatially common and consistent brain networks. The application of this hybrid temporal and spatial sparse representation framework in a natural stimulus fMRI dataset achieved promising results.

2. MATERIALS AND METHODS

2.1. Overview

The overview of our framework is illustrated in Fig.1. In the first stage, the whole-brain fMRI signals of each individual brain (the first and second rows in Fig.1a) is sparsely represented, as similarly performed in [10, 11]. This step results in a collection of atomic temporal signal components (the third row in Fig.1a) and their associated spatial distributions (the fourth row in Fig.1a). It is particularly noted that the atomic dictionary components across individual brains are significantly different due to the intrinsic variability and a variety of possible noise sources, even though the subjects watched the same set of video streams. In comparison, the atomic dictionary components in sparse representation of task-based fMRI data are much more consistent as reported in [10, 11]. Actually, this is the major difference between natural stimulus fMRI data and

task-based fMRI data when the whole-brain sparse representation method is employed, which motivated us to apply the second stage of spatial sparse representation of the coefficient maps associated with those atomic temporal components across different brains, as illustrated in Fig.1b. Specifically, all of the spatial maps are aggregated into the same template brain space as a big data matrix and then sparsely represented (first row of Fig.1b). This step results in the atomic spatial components, as shown in the second row of Fig.1b, which essentially stand for the most common and prominent spatially-referenced networks in the brain. In this paper, these networks are considered as the consistent spatial networks across different brains in natural stimulus fMRI dataset.

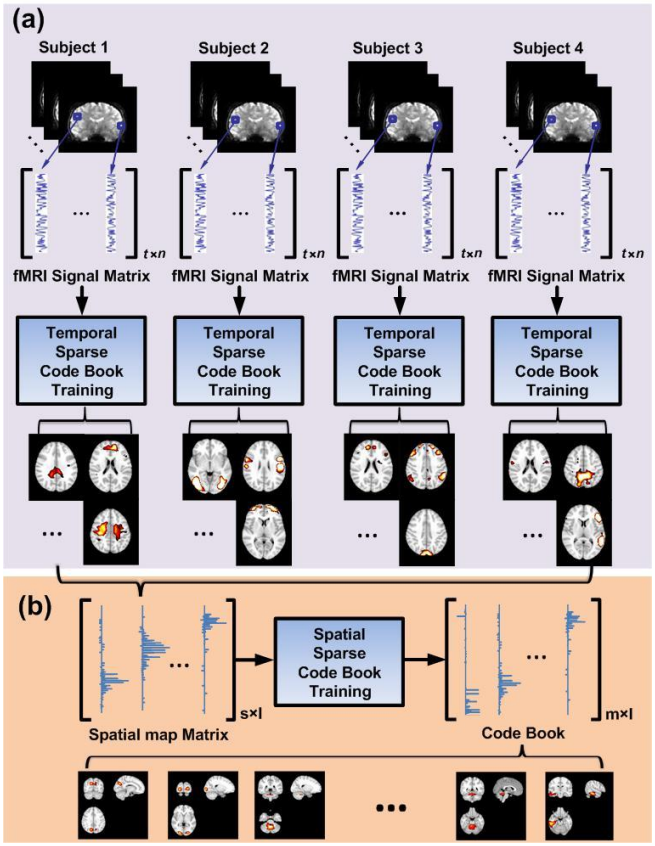

Fig.1. The flowchart of our hybrid sparse representation framework. (a) Temporal sparse representation. Each individual's whole-brain fMRI signals are sparsely represented. (b) Spatial sparse representation. Spatial coefficient distribution maps of temporal components across different brains are sparsely represented.

2.2. Data and Preprocessing

For fMRI natural stimuli, we randomly selected 32 video shots from the TRECVID [12], which is a standard video collection in the multimedia analysis field. Three semantic categories are covered these video shots including sports, advertisement and weather reports. We made the video shots into 4 clips, each of which is around 11 minutes. The video clips were then presented to 4 healthy university students for fMRI brain imaging at the Bioimaging Research Center (BIRC) of The University of Georgia. Details of fMRI scan and data preprocessing are referred to our prior study [13].

2.3. Hybrid Temporal and Spatial Sparse Representation

As outlined in Fig.1, our study contains two parts: the first is temporal sparse representation (Fig.1 (a)), and the second part is spatial sparse representation (Fig.1 (b)). Sparse representation theory is widely used nowadays [15]. Specifically, the temporal sparse representation in this work can be written as:

$$\mathbf{y} = \sum_{i=1}^{\mathbf{k}} \alpha_i * D_i = \alpha * D \quad _{D\epsilon\mathbb{R}^{\mathbf{t}\times\mathbf{k}},\alpha\epsilon\mathbb{R}^{\mathbf{k}\times\mathbf{n}}} \tag{1}$$

where $\mathbf{y}$ is the $\mathbf{t}\times\mathbf{n}$ fMRI signal matrix in ($\mathbf{t}$ is the signal length, $\mathbf{n}$ is the number of whole-brain voxels) for each individual, as shown in the first and the second row of Fig.1 (a). α is the coefficient matrix, in which α_k indicates the contribution of the k-th atom in the reconstruction of original signal $\mathbf{y}$. D denotes the dictionary, where each column of it is presumably the dominate hidden functional activity time series that constitute the whole-brain fMRI data.

We project each coefficient vector in the coefficient matrix back to the fMRI image space [10, 11], which results in a spatial map. The classic t-statistics is applied to convert a spatial map to a T-statistics map. For the purpose of group analysis, the T-statistics maps are aligned to the MNI brain template using the nonlinear registration tool FNIRT in FSL [16]. These steps are akin to the methods in [13, 14].

In comparison with our prior works that performed temporal sparse coding [10, 11], the major methodological innovation in this paper is the spatial sparse representation (Fig.1(b)), which is applied after the temporal sparse representation. This step aims to infer spatially common and consistent brain networks. Here, the collection of spatial maps from each individual obtained in the first step of temporal sparse coding (the first row of Fig.2) will be put together to form another data matrix to perform sparse representation:

$$S = D_{spa}\alpha_{spa} + \varepsilon \tag{2}$$

where $\mathbf{S}$ stands for spatial maps from all the brains. ε is the residual. α_{spa} is the coefficient matrix, D_{spa} is the collection of spatial dictionary. In this way, common spatial patterns will be learned. Each column of D_{spa} is a common spatial distribution. We empirically set the size of the spatial dictionary to 100 in our study with the consideration of the total number of networks in the human brain. We infer inter-subject correspondence between the temporal dictionaries by looking up the coefficient matrix in the spatial sparse representation. Briefly, for each atom in the spatial dictionary, the maximal coefficient from each part in the row of spatial coefficient matrix (the third row of Fig.2) is considered as the individual's best-fitted distribution of the atom. With the established correspondences, we

quantitatively measure the spatial consistency and temporal consistency of the atoms in the spatial dictionary.

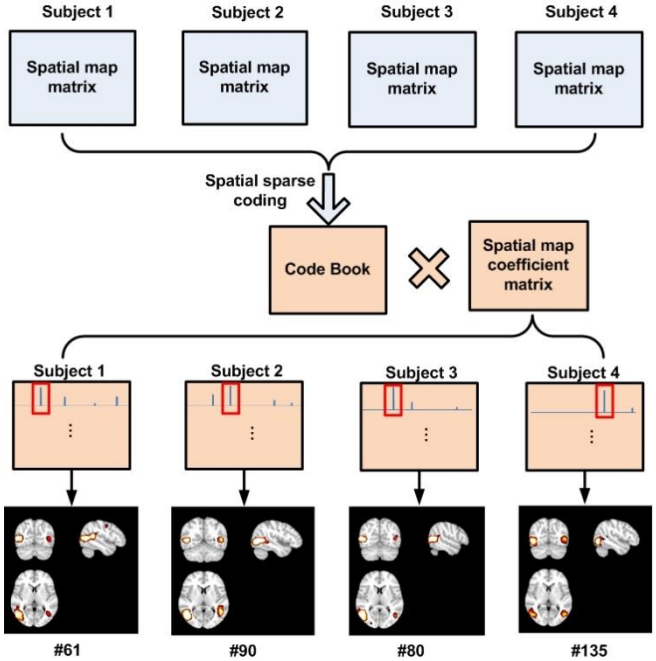

Fig.2. Steps for establishing correspondence across spatial patterns in different individuals. The maximum in the coefficient vector is highlighted by red rectangle, whose corresponding spatial patterns (shown to the bottom) are considered as group-wise consistent sub-networks.

Specifically, the spatial consistency is calculated as the spatial overlap rate over each individual's common spatial map:

$$overlap = S_{overlap} / S_{all} \quad (3)$$

where $S_{overlap}$ denotes the area of overlap for all common spatial distribution and S_{all} stands for the union area of common spatial maps.

The temporal consistency is calculated as equation:

$$temporal\ consisitency = \lambda_1 / S_\lambda \quad (4)$$

Here, λ_1 denotes the first eigenvalue in principal component analysis (PCA) applied on the collected atoms, which are based on the same spatial distribution, in each individual's temporal dictionary and S_λ denotes the sum of all the eigenvalues.

3. RESULTS

The application of the methods in section 2.3 on the dataset in section 2.2 obtained 100 spatial dictionary atoms. The spatial consistency of the atoms in the spatial dictionary is shown in Fig.3 in descending order. The top six most spatially consistent networks are shown in Fig.4. It can be seen that the visual (Fig.4#4, #6), motor (Fig.4#3), auditory (Fig.4#5) networks are commonly involved in the comprehension of natural stimuli, which are quite reasonable. These results show that spatially consistent networks can be inferred across subjects and fMRI sessions regardless of intrinsic variability and noises sources, suggesting the effectiveness of our hybrid sparse representation framework.

The temporal consistency of dictionary atoms is shown in Fig.5 in descending order of spatial consistency. It is not a surprise that there are temporally consistent and inconsistent atoms, as highlighted by the color arrows respectively. Fig.6(a) and shows an exemplar brain network with low temporal consistency (as highlighted by the green arrow in Fig.5). Fig.6(b) shows a brain network with low spatial consistency but high temporal consistency (as highlighted by the red arrow in Fig.5). However, there are networks with both spatial and temporal consistencies, as shown in Fig.6(c) for an example (as highlighted by the orange arrow in Fig.5). It turns out that this spatial map is the right Broca's area (Brodmann area 45).

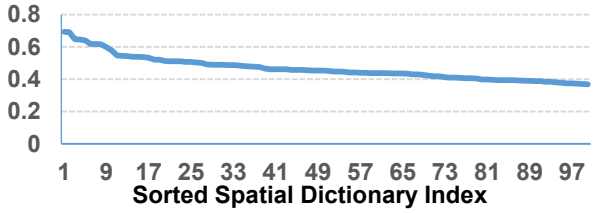

Fig.3. Overlap ratios of the 100 learned spatial dictionary atoms in descending order.

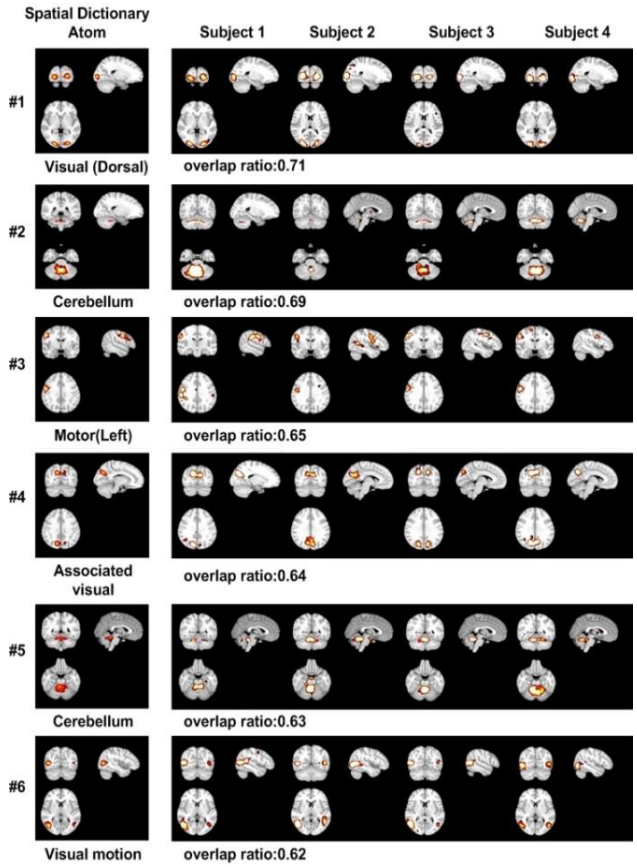

Fig.4. Top six spatially consistent networks (each row).

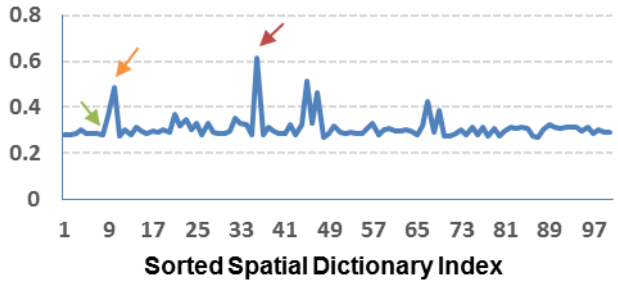

Fig.5. Temporal consistency of the sorted dictionary atoms in descending order of spatial consistency.

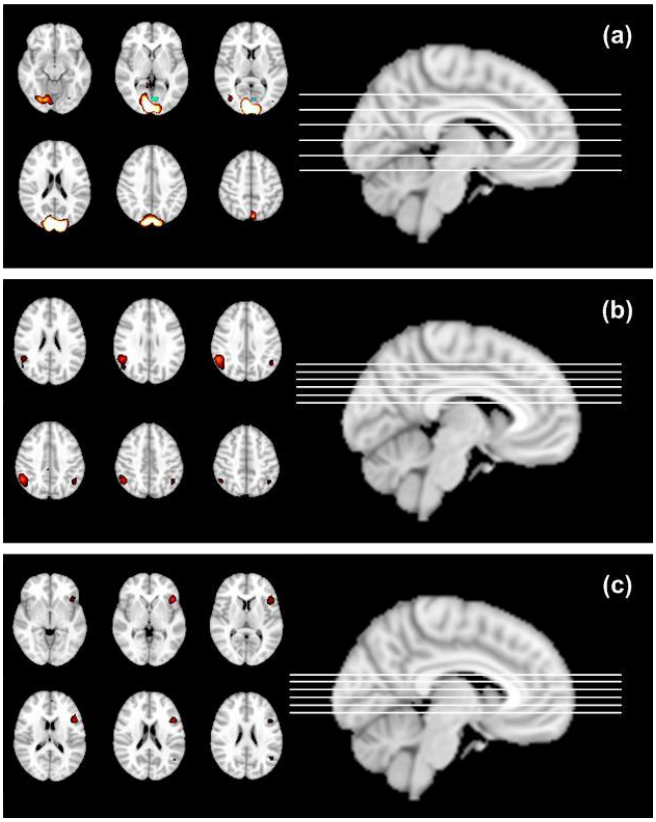

Fig.6. (a) Temporally inconsistent network (atom #9, as highlighted by the green arrow in Fig.5). (b) Temporally consistent but spatially inconsistent network (atom #36, as highlighted the red arrow in Fig.5). (c) Both temporally and spatially consistent network (atom #10, as highlighted the orange arrow in Fig.5)

4. DISCUSSION AND CONCLUSION

Our work demonstrated that hybrid temporal and spatial sparse representation can be used to decompose whole-brain natural stimulus fMRI signals into meaningful network activities. Importantly, consistent spatial distributions of such networks across different subjects can be discovered, suggesting the existence of common networks that are frequently involved in various situations and across individual brains. This result from natural stimulus fMRI dataset, instead of task-based fMRI dataset, might indicate the common functional brain architecture for natural stimulus comprehension as previously revealed by our HAFNI (holistic atlases of functional networks and interactions) system [11]. Therefore, our pilot work in this paper could serve as a start point for future exploration of the interactions between external multimedia stimuli and functional brain response in the future, as outlined in [17].

5. REFERENCES

[1] K. J. Friston, "Modalities, modes, and models in functional neuroimaging," *Science*, 326(5951), pp. 399, 2009

[2] J. V. Haxby, M. I. Gobbini, M. L. Furey et al., "Distributed and overlapping representations of faces and objects in ventral temporal cortex," *Science*, 293(5539), pp. 2425-2430, 2001.

[3] Bartels, and S. Zeki, "Brain dynamics during natural viewing conditions - a new guide for mapping connectivity in vivo," *Neuroimage*, 24(2), pp. 339-349, 2005.

[4] M. Pearce, and M. Rohrmeier, "Music cognition and the cognitive sciences," *Topics in cognitive science*, 4(4), pp. 468-484, 2012.

[5] U. Hasson, R. Malach, and D. J. Heeger, "Reliability of cortical activity during natural stimulation," *Trends in cognitive sciences*, 14(1), pp. 40-48, 2010

[6] A. Bartels, and S. Zeki, "The chronoarchitecture of the human brain--natural viewing conditions reveal a time-based anatomy of the brain," *Neuroimage,* 22(1), pp. 419-33, 2004.

[7] K.J. Friston, et al. "Statistical parametric maps in functional imaging: a general linear approach". *Human Brain Mapping* 2(4), pp. 189–210, 1994.

[8] Kauppi, Jukka-Pekka, et al. "Inter-subject correlation of brain hemodynamic responses during watching a movie: localization in space and frequency." *Frontiers in neuroinformatics* (4), 2010.

[9] B.A. Olshausen& D.J.Field, "Sparse coding of sensory inputs". *Current opinion in neurobiology*, 14(4), pp. 481-487, 2004

[10] J. Lv, X. Jiang, X. Li, *et al.*, "Sparse representation of whole-brain fMRI signals identification of functional networks," *Medical Image Analysis*, 20(1), pp. 112-134, 2014

[11] J. Lv, X. Jiang *et al*., "Holistic Atlases of Functional Networks and Interactions Reveal Reciprocal Organizational Architecture of Cortical Function," in *IEEE TBME*, 62(4), pp. 1120-1131, 2015

[12] X. Hu, K. Li, J. Han, *et al.*, "Bridging the semantic gap via functional brain imaging," *IEEE Transactions on Multimedia,* 14(2), pp. 314-325, 2012

[13] C. Lv, et al. "Exploring consistent functional brain networks during free viewing of videos via sparse representation." In *ISBI2014*, pp. 349-352, 2014

[14] J. Lv, *et al*., "Assessing Effects of Prenatal Alcohol Exposure Using Group-wise Sparse Representation of FMRI Data," *Psychiatry Research: Neuroimaging*, *in press*, 2015.

[15] J. Mairal, F. Bach, J. Ponce *et al.*, "Online learning for matrix factorization and sparse coding," *Journal of Machine Learning Research,* 11, pp. 19-60, 2010

[16] M. Jenkinson, C.F. Beckmann, T.E. Behrens, M.W. Woolrich, S.M. Smith. FSL. *NeuroImage*, pp. 782-90, 2012

[17] T. Liu, X. Hu, X. Li, *et al.*, Merging Neuroimaging and Multimedia: Methods, Opportunities and Challenges, *IEEE Transactions on Human-Machine Systems*, pp. 1-11, 2014